An Investigation of the Coefficient of Variation Using the Dissipative Stochastic Mechanics Based Neuron Model

Sinan Hazim Naife

Submitted to the
Institute of Graduate Studies and Research
in partial fulfillment of the requirements for the Degree of

Master of Science
in
Computer Engineering

Eastern Mediterranean University
August 2013
Gazimağusa, North Cyprus

Approval of the Institute of Graduate Studies and Research

Prof. Dr. Elvan Yılmaz
Director

I certify that this thesis satisfies the requirements as a thesis for the degree of Master of Science in Computer Engineering.

Assoc. Prof. Dr. Muhammed Salamah
Chair, Department of Computer Engineering

We certify that we have read this thesis and that in our opinion it is fully adequate in scope and quality as a thesis for the degree of Master of Science in Computer Engineering.

Prof. Dr. Marifi Güler
Supervisor

Examining Committee

1. Prof. Dr. Marifi Güler

2. Assoc. Prof. Dr. Işik Aybay

3. Asst. Prof. Dr. Adnan Acan

ABSTRACT

In recent years, it has been argued and shown experimentally that ion channel noise in neurons can have profound effects on the neuron's dynamical behavior. Most profoundly, ion channel noise was seen to be able to cause spontaneous firing and stochastic resonance.

A physical approach for the description of neuronal dynamics under the influence of ion channel noise was proposed recently through the use of dissipative stochastic mechanics by Guler in a series of papers. He consequently introduced a computational neuron model incorporating channel noise. The most distinctive feature of the model is the presence of so-called the renormalization terms therein. This model exhibits experimentally compatible noise induced transitions among its dynamical states, and gives the rose-Hindmarash model of the neuron in the deterministic limit.

In this thesis, statistics of coefficient of variation will be investigated using the dissipative stochastic mechanics based neuron model.

Keywords: Ion Channel Noise, Stochastic Ion Channels, Neuronal Dynamic, Hindmarsh-Rose Model, Dissipative Stochastic Mechanism Model

ÖZ

Son yıllarda, nöronlardaki ion kanal gürültüsünün nöron dinamiği üzerinde hayati etki yapabildiği deneysel olarak da kanıtlanmıştır. Bu kapsamda, kendi kendine ateşleme ve stokastik rezonans en çarpıcı bulgulardır.

İyon kanal gürültüsü altındaki nöron dinamiği, fiziksel bir yaklaşım olan disipatif stokastik mekanik kullanarak Güler (2006, 2007, 2008) tarafından çalışılmış ve modellenmiştir. Sonsuz zar büyüklüğü limitinde Rose-Hindmarsh modeline dönüşen bu disipatif stokastik mekaniğe dayalı modelin en önemli özelliği renormalizasyon terimleri içermesidir. Bu tezde, Rose-Hindmarsh tipi zarlarda iyon kanal gürültüsü için geliştirilmiş olan yukarıdaki model kullanılarak ateşleme dinamiği üzerinden değişkenlik katsayısı hesaplamaları yapılmıştır.

Anahtar Kelimeler: İyon kanal gürültüsü, Stokastik iyon kanalları, Nöronal Dinamik, Rose-Hindmarsh Modeli, Disipatif stokastik mekanik modeli

I dedicate this thesis to my mother, father, uncle, my lovely aunt, two sisters and brother, and to all my friends.

ACKNOWLEDGMENTS

In the name of greatest All mighty ALLAH who has always bless us with potential knowledge and success.

I sincerely acknowledge all the help and support that I was given by Prof. Dr. Marifi Güler whose knowledge, guidance, and effort made this research go on and see the light.

My deep gratitude to my mother and father for the support, effort, pain, and patience whom I own the success of my life to them. Special thanks go to my friends Humam M. jassim, Mohammed Namik, , haydar m.jasim, Liwaa Hussein, Ahmed Mahmoud, Anas Qasim, Mustafa ibraheem, Ghassan Qas Marrogy and to all my friends for their help and support.

TABLE OF CONTENTS

LIST OF FIGURES

LIST OF TABLES

Chapter 1

INTRODUCTION

Neurons exhibit electrical action which is in nature known to be stochastic (Faisal 2008). The main source of stochasticity is the external noise from the synapses. Still the interior noise, which participates to the gating probabilistic nature of the ion channel, and also it can have important effects on the neuron's dynamic performance as displayed by the experimental studies (Kole 2006; Jacobson et al. 2005; Sakmann and Neher 1995) and by the numerical simulations or theoretical researches (Chow and White 1996; Fox and Lu 1994; Schmid et al. 2001; Schneidman et al. 1998).

Neuronal dynamics under the effect of channel fluctuation is usually modeled with stochastic differential equations acquired by using some vanishing white-noise conditions into the fundamental deterministic equations (Fox and Lu 1994). The dissipative stochastic mechanics (DSM neuron) based neuron model raised by Güler (2006, 2007, 2013), is a special case of this. The DSM model has some forms of functionality named the renormalization terms, as well as some vanishing white-noise conditions in the activity equations. The DSM model has been studied in numerical detail for its time independent input current's dynamics (Güler 2008, 2013); it was established that the corrections of renormalization increases the changes in behavior from quiescence to spiking and from tonic firing to bursting. It was further established that the existence of renormalization corrections can result in faster temporal synchronization of the electric coupled

consecutive discharges of two neuronal units (Jibril and Güler 2009). In this thesis, the DSM model is investigated in the situation of noise fluctuating input currents and concentrates on what role the renormalization terms and noise could have on the spiking rates and the spike coherence values.

In neural membrane patches, spontaneous activity phenomenon occurs (in the case of repeating spikes or bursts) and the reason about that is the internal noise from ion channels; these present during numerical simulations of channel dynamics and theoretical investigations ((DeFelice, 1992); (Strassberg, 1993); (Lu, 1994); (Chow, 1996); (Rowat, 2004); (Güler, 2007); (Güler, 2008); (Güler, 2011) (Güler, 2013)); besides ,those experiments have shown the happening of stochastic resonance and the coherence of the procreated spike trains (Almassian A., 2011); (Jassim H. M., 2013) (Jung, 2001); (Schmid, 2001); (Özer, 2006)). Even when the numbers of ion channels are large, channel fluctuations might become critical near to the action potential threshold (Abdulmonim M. N., 2013); (Schneidman, 1998); (Rubinstein, 1995)); the small number of ion channels that are open at the action potential threshold assigned the accuracy of timing of action potential. Also it has been clarified that ion channel noise affects the spike generation in axons ((Faisal A. A., 2007); (Ochab-Marcinek, 2009)). The renormalization of the fluctuations in a number of open gates not only affects the neuron behavior, but also the attendance of a multiple number of gates in every ion channel. Moreover, this effect may indicates to an important act in cell activity in state of having coherence membrane in size (Güler, 2013).

Chapter 2

NEURON STRUCTURE

2.1 Morphology and Structure

Neurons are a specific kind of cells found in the human brain they're unique in generating electrical signals in reaction to chemical as well as other inputs. A normal nerve cell will be divided into three parts: the soma or cell body dendrites and axon. Dendrites receive inputs from other neurons cell and propagate it for the soma. The axon transmits the neuronal output to other cells. The dendrites structure is like a branch of a tree increases area cell from the branching structure which improves the capability of the neuron to receive a number of other cells through synapses connections. Figure1 explains details and structure for that neuron. Axons by single neurons traverse big brain's fractions or sometimes from the system. It is estimated that cortical neurons typically send about 40 mm of axon and also have approximately 4 mm of total dendritic cable into their structural dendritic trees. The axon makes an average of 180 synaptic connections to neurons per mm of length during the dendritic tree receives, normally 2 synaptic inputs per μm. The cell body or soma of the typical cortical neurons ranges in diameter from about 10 to 50 μm (Abbot, 2002).

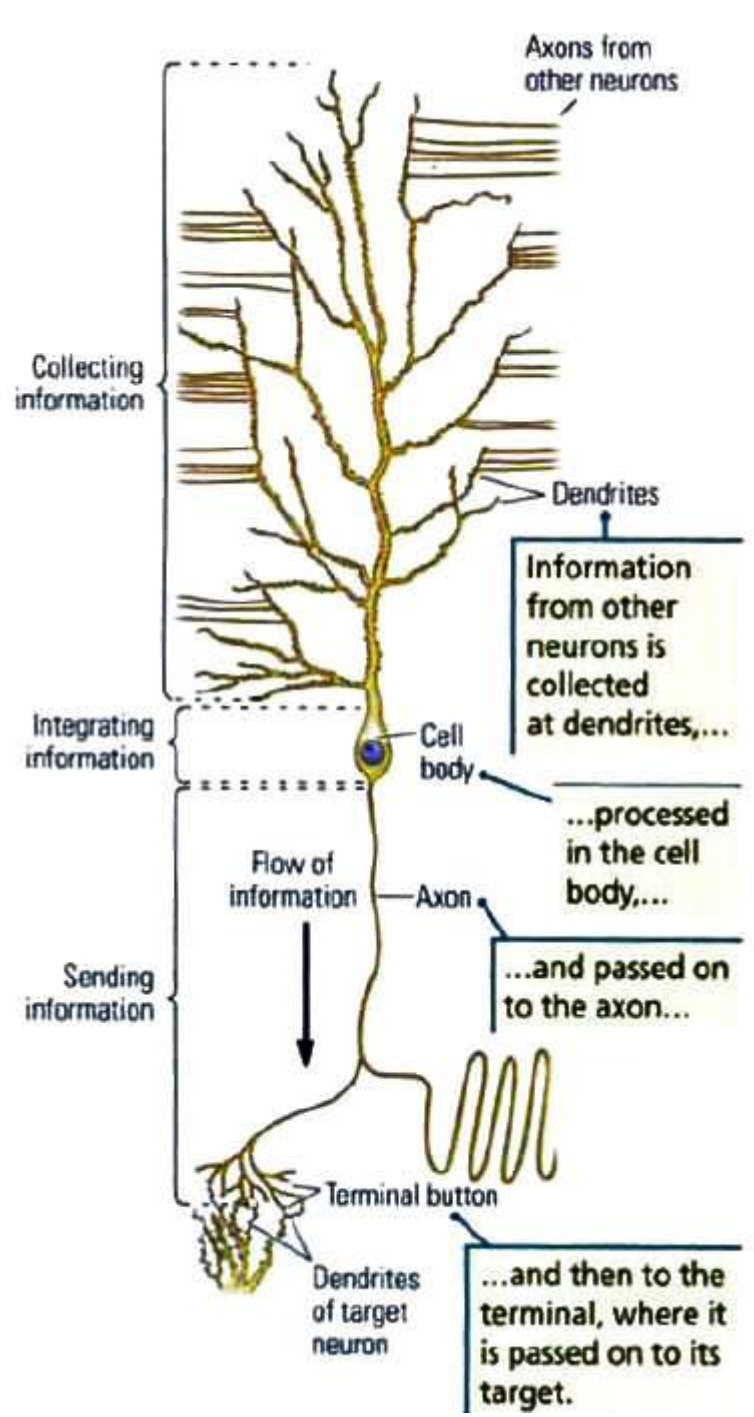

Figure 1: Two Interconnected Cortical Pyramidal Neurons (Izhikevich, 2007)

2.1.1 What is a Spike?

The communication mean among the neurons in simple a current pulse is called as spike. Neurons normally receive 10,000 ---from another through the synapse. If the signal is received on the other neurons, this signal causes modifications to the existing of the transmembrane. The existing coming synapse is referred to as the post synaptic potentials (PSPs), little PSPs are generated from tiny current, large PSPs are generated in time when current considerably high. The voltage sensitive channel is inserted a neuron, these channels are resulting to generation of action potential or spike (Izhikevich, 2007).

2.1.2 Membrane Proteins

Protein is an essential part of the cell membrane that transports molecules across it. These proteins play a substantial part in determining the function of neurons. Finding out how membrane proteins work is useful for understanding many functions of neurons. We describe many types of membranes proteins that help in transporting substances around the membrane like channels, gates, and pumps.

2.1.2.1 Channels

Some membranes proteins are shaped in this type of method which create channels, or holes, across that substance can pass. Different proteins with various sized holes permit different substances to go in or depart the cell. Protein molecules assist as channels for predominantly sodium (Na+), potassium (K+), calcium (Ca2+), and chloride (Cl−) ions.

2.1.2.2 Gates

An essential feature of a little protein molecules is the skill too change shape. Some gates work by changing form after one more chemical binds to them. In such cases, the embedded protein molecule deeds like a door lock. After having a key of the appropriate size and form is inserted in it and turned, the locking device adjusts the shape and becomes activated. Other gates change shape when certain conditions in their environment, for example electrical or temperature, change.

2.1.2.3 Pump

Sometimes, a membrane protein deeds like a pump, a transporter molecule that needs power to move substances over the membrane. For example there is protein that adjusts its form to impel Na+ ions in one direction and K+ ions in the other direction. Countless substances are transported by protein pumps. Channels, gates, and pumps play an essential role in a neuron's ability to convey information.

2.1.3 Synapse

Synapses are shaped such as a junction amid two consecutive neurons after the axon of sensory neuron is related to the efferent one and supplies a method to communicate the information to other cell. Axons terminate at synapses whereas the voltage transient of the action potential opens ion channels producing an influx of Ca2+ that leads towards the discharge of neurotransmitter. The neurotransmitter binds to receptors at the gesture consenting or postsynaptic side of the synapse provoking ion-conducting channels to

open. Reliant on the nature of the ion flow, the synapses can have an excitatory, depolarizing, or an inhibitory, normally hyperpolarizing, result on the postsynaptic neuron (Abbot 2002).

Synapses are not randomly distributed above the dendritic surface. In finish, inhibitory synapses are more proximal than excitatory synapses, although they are additionally present at distal dendritic spans and, after being present, on some spines in combination alongside an excitatory input (Segev in Bower and Beeman 2003). In countless systems (e.g., pyramidal hippocampal cells and cerebellar Purkinje cells), provided input basis is preferentially mapped onto a given lifetime of the dendritic tree, rather being randomly distributed above the dendritic surface. Electron micrographic pictures of synapses in real neurons are shown in figure 2.

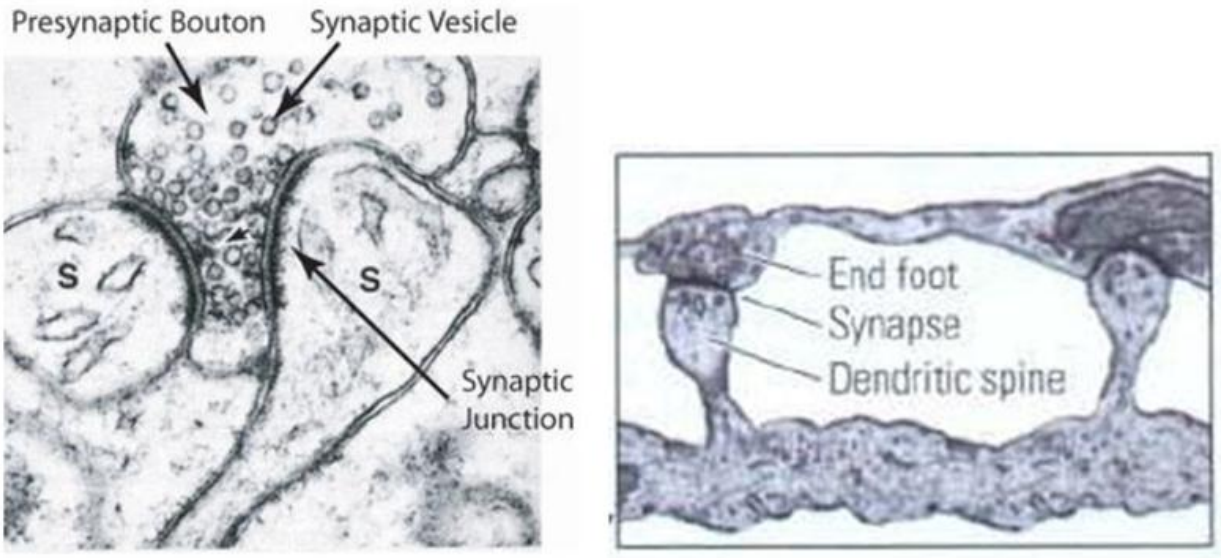

Figure 2: Synapses Examples: **(A)** Electron Micrograph of Excitatory Spiny Synapses (s) Shaped on the Dendrites of a Rodent Hippocampal Pyramidal Cell. (B) An Electron Micrographic Figure Captured the Synapse Formed Where The Terminal Bottom of One Neuron Meets a Dendritic Spine on a Dendrite of Another Neuron (Kolb and Whishaw 2009).

2.2 Membrane Potential and Neuron Electrical Activity

Membrane potential is described as difference in electrical potential between the inside of a neuron and the surrounding ECF. Under resting conditions, the possibility inside the cell membrane of a neuron is around -70 mV relative to that of the encompassing bath. This voltage, however, is conventionally assumed to become 0 mV for convenience and the cell is claimed to be polarized in this state. This potential is in cell matches that out from the cell. This membrane potential difference is sustained by ion pumps based in the cell membrane by maintaining concentration gradients. For example, Na+ is much more concentrated outside a neuron than inside it and also the concentration of K+ is significantly higher inside neuron in comparison to the extracellular fluid. Therefore, ions flow into and out of the cell because of both voltage and concentration gradients

during the entire state transition of cell. Current, in the form of electropositive ions flowing out of the cell (or electronegative ions flowing into the cell) through open channels helps make the membrane potential more negative, a process called hyperpolarization. Current flowing into the cell changes the membrane possibility to less negative and even positive values. This is known as depolarization. When a neuron is depolarized sufficiently large to increase the membrane potential above a threshold level, an optimistic feedback process is began and the neuron generates an action potential. An action potential is usually roughly 100 mV fluctuations in the electrical potential across the cell membrane that takes about 1ms. Once an action potential occurs it can be impossible to initiate another spike following the previous one and this is known as the total refractory period. The importance of action potential in the fact that unlike subthreshold fluctuations that attenuate over distance of at most 1 millimeter they are able to propagate over large distances without attenuation along axon processes (Dayan and Abbot 2002). Figure 3 depicts the voltage dynamic of a neuron during an action potential even though it is synthesized by corresponding ion channel activities throughout an action potential. Therein figure the resting potential is in its real value -70 mV.

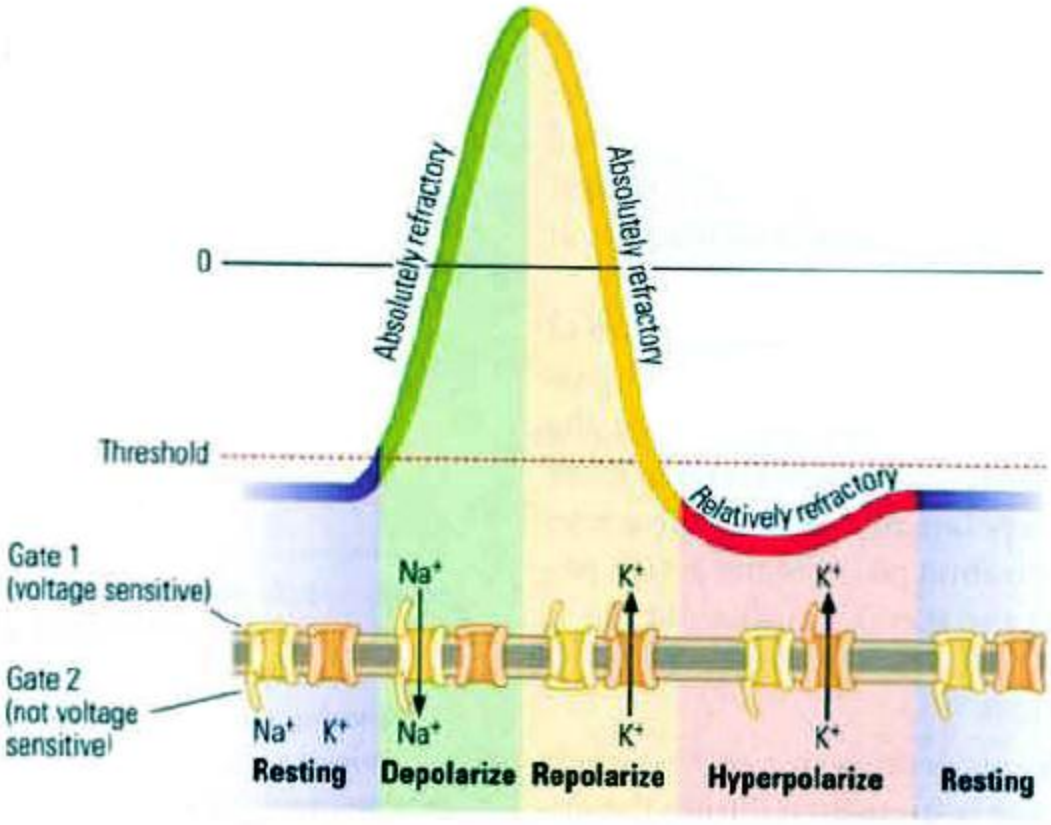

Figure 3: Phases of an Action Potential Initiated by Changes in Voltage Sensitive Sodium and Potassium Channels, an Action Potential Begins with a Depolarization (gate 1 of the Sodium Channel Opens and then Gate 2 Closes). The Slower-opening Potassium Channel Contributes on Re-polarization and Hyper-polarization until the Resting Membrane Potential is Restored (Kolb and Whishaw 2009).

Chapter 3

HODGKIN - HUXLEY EQUATIONS

Over the years, many neurons model have been located and developed according to the purpose they used for. Furthermore, the diversity of the models found is determined by the actual biophysical model with regard to structure. Hodgkin – Huxley (HH) is the more applicable model up to now, also one of the simplified models utilized in the experiments with this thesis: the Hindmarsh-Rose model (HR). However, modeling technic of neural excitability has been influenced by the monument work of Hodgkin-Huxley (1952). In this part, Hodgkin – Huxley model and also the Hindmarsh-Rose model (HR) are going to be briefly explained.

In this chapter we briefly handles the two Hodgkin-Huxley model and Hindmarsh-Rose model (HR), after that we will concentrate on the most recent dissipative stochastic mechanics (DSM) set up from the neuron model that accomplishes the deterministic condition of the dynamics of HR model and it can be focused and experimented in this section .

3.1 The Hodgkin-Huxley Model

Depending on experimental research done on an axon of giant squid using space clamp and voltage clamp techniques, Hodgkin and Huxley (HH) (1952) explained that the current passing through the axon of a squid has only two major ionic elements, I_{Na} and I_k (sodium and potassium channel equivalent elements). The membrane potential V_m has influence on these currents significantly. Accordingly, they developed from their observation a mathematical model to create a model that is still one of the most important model and depending on it, scientists developed lots of realistic neural models (Hodgkin and Huxley 1952).

According to the style of Hodgkin – Huxley that they explain the characteristics of electrical nerve patch membrane, as a possible equivalent circuit. In this patch all of the current across is manufactured of two basic sections: charging membrane capacitance may be the first one and the second is come with transport a particular type of ions via the membrane. Moreover the currents of ion are made of three unique elements, the potassium, sodium, and also the chloride. The current of sodium I_{Na}, the current of potassium I_K and the current of leakage I_L which can be related to chloride.

Depending on Hodgkin-Huxley electrical circuit the equation are going to be:

$$C_m \frac{dV_m}{dt} + I_{ion} = I_{ext} \qquad (1)$$

Where

C_m is membrane capacitance

V_m is membrane potential

I_{ext} is an externally current

I_{ion} is the ionic current

The currents of ions through the membrane could be found using equation as follow

$$I_{ion} = \sum_i I_i \qquad (2)$$

$$I_i = g_i(V_m - E_i) \qquad (3)$$

The currents from the equation number (3) each one is related with a conductance g_i with reactive potential E_i depending on H-H the currents of ion that over the membrane inside the I_{ion} squid giant axon is actually three: I_{Na} (current of sodium), I_K (current of potassium) and also a current of leakageI_L, as display in the following equations .

$$I_{ion} = I_{Na} + I_K + I_L \qquad (4)$$

$$I_{Na} = g_{Na}(V_m - E_{na}) \qquad (5)$$

$$I_K = g_K\,(V_m - E_K) \qquad (6)$$

$$I_L = g_L\,(V_m - E_L) \qquad (7)$$

The conductance g_i (g_L, g_K, g_{Na}) are created from the mixed impact of a big amount of tiny ion channels. The meaning I_{ion} is basically such as the amount of open up physical

gates. These types of gates usually control the passage of ions through the channel. The ions can transfer through the channel to the time that the channel is open; this channel is assumed to be open only when the entire gates of this channel has been permissive condition.

3.1.1 The Ionic Conductance

Ions can pass through the channel and it is open when all of the gates for a particular channel are in the permissive state. The formal assumptions used to describe the potassium and sodium conductance empirically achieved by voltage clamp experiments.

$$g_K = \bar{g}_K n^4 \qquad (8)$$

$$g_{Na} = \bar{g}_{Na} m^3 h \qquad (9)$$

where n, m and h are variable's dynamics of the ion channel gate that will be shown later on, $\bar{g}_i$ is a constant with the scales of conductance per cm^2 (remember that n is between 0 and 1, consequently, the maximum conductance value is needed ($\bar{g}_i$) to normalize the result).The dynamic of n, m, and h are listed below:

$$\dot{n} = \frac{dn}{dt} = \alpha_n(1-n) - \beta_n n \qquad (10)$$

$$\dot{m} = \frac{dn}{dt} = \alpha_m(1-m) - \beta_m m \qquad (11)$$

$$\dot{h} = \frac{dh}{dt} = \alpha_h(1-h) - \beta_h h \qquad (12)$$

where α_x and β_x are rate constants, that fluctuate with voltage but not with time, *n* is a non-dimensional variable that can fluctuate between 0 and 1 and shows the individual gate probability of being in the permissive state.

The potential of membrane V_m (in voltage clamp test) starts usually from the resting period (V_m = 0) and followed by immediate arise to achieve V_c. In order to find equation (11) over the following the following exponential may be used.

$$x(t) = x_\infty(V_c) - \big(x_\infty(V_c) - x_\infty(0)\big)\exp(-t/\tau_x) \quad (13)$$

$$x_\infty(0) = \alpha_x(0)/\alpha_x(0) + \beta_x(0) \quad (14)$$

$$x_\infty(V_c) = \alpha_x(V_c)/\alpha_x(V_c) + \beta_x(V_c) \quad (15)$$

$$\tau_x(V_c) = [\alpha_x(V_c) + \beta_x(V_c)]^{-1} \quad (16)$$

In these equations x stands for the time which depends on all the n, m and h (gate variable), as a result the formula becomes simpler, all of the values of the gate variable $x_\infty(0) = 0$ at the resting condition and $x_\infty(V_c) = V_c$). Although τ_x here stands for the time needed to let x_∞ reach the steady state in the event the voltage of x_∞ achieve V_c .

The rate constant α_i β_i measured in H-H as function with V as follows:

$$\alpha_i = \frac{x_\infty(V)}{\tau_n(V)} \quad (17)$$

$$\beta_i = \frac{1-x_\infty(V)}{\tau_n(V)} \quad (18)$$

As pointed previous to inside the, i is for n, m, and h. These below equations are for that rate constant α_i β_i, and could be determined from the following:

$$\alpha_n(V) = \frac{0.01(10-V)}{\exp\left(\frac{10-V}{10}\right)-1} \quad (19)$$

$$\beta_n(V) = 0.125 \exp\left(-\frac{V}{80}\right) \quad (20)$$

$$\alpha_m(V) = \frac{0.1(25-V)}{\exp\left(\frac{10-V}{10}\right)-1} \quad (21)$$

$$\beta_m(V) = 4 \exp\left(-\frac{V}{18}\right) \quad (22)$$

$$\alpha_h(V) = 0.07 \exp\left(-\frac{V}{20}\right) \quad (23)$$

$$\beta_h(V) = \frac{1}{\exp\left(\frac{30-V}{10}\right)+1} \quad (24)$$

All of (V) and $\beta(V)$ describe the transition rates between open and closed states of the channels.

3.2 The Hindmarsh Rose Model

Although Hodgkin-Huxley (HH) model can depict the neural dynamics of spiking neuron to a substantial range, in large models the Hodgkin-Huxley (HH) bursting model might be difficult. The axon of squid neuron have been researched by Hodgkin-Huxley who find out it have both of them Na and K conductance, although there are other conductance types contribute inside the (HH) bursting model that will increase the complexity inside the model.

FitzHugh and Nagumo (1961) observed separately in HH equations, that the improvements both in membrane potential $V(t)$ and sodium activation $m(t)$ happened in similar time scales during an action potential, whereas the change in sodium inactivation $h(t)$ and also potassium activation $n(t)$ are similar, although slower time scales. It can display the simulation of the model spiking behavior in the following equations:

$$\dot{x} = a(y - f_1(x) + I) \qquad (25)$$

$$\dot{y} = b(g_1(x) - y) \qquad (26)$$

Where x stands for membrane potential and y indicates the recovery parameter. $f_1(x)$ is represented with cubic function, $g_1(x)$ with linear function, variables a and b are time constants and that $I(t)$ is the external current used or clamping while time function t. Hindmarsh-Rose taken advantage of the FitzHugh-Nagumo model to improve their model, that was a simple version of the (H-H) equations and substituted the linear function g(x) with a quadratic function so the model long interspaces interval can

achieve rapid firing. Figure (4) shows the diagram of null-cline of the Hindmarsh-Rose model (Hindmarsh J.L. and Rose R.M 1982).

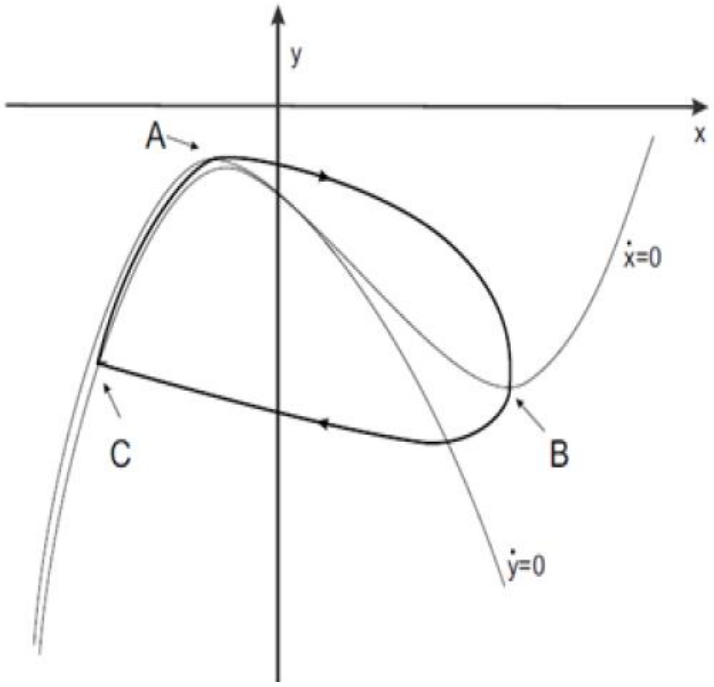

Figure 4: The 1982 HR model phase plane representation. Null-clines $\dot{\mathbf{x}}$= 0, $\dot{\mathbf{y}}$= 0 (thin lines) and firing limit-cycle (thick line). Design for one equilibrium node (Steur 2006).

HR model needs several equilibrium points to generate burst firing reaction. Generally the condition of sub-threshold stable resting can have one point then one point in the cycle of firing limit. To make the null-clines meet and bring additional points of equilibrium, a small deformation was necessary. The controlling equations were altered to satisfy the requirements as proven in the following equations:

$$\dot{x} = y - f(x) + I \qquad (27)$$

$$\dot{y} = g(x) - y \qquad (28)$$

where the $f(x) = x^3 - 3x^2$ inside the simple form of $f(x)$ in HR design, , $g(x) = 1 - 5x^2$. The phase plane analysis of the given equations is shown in Figure 5.

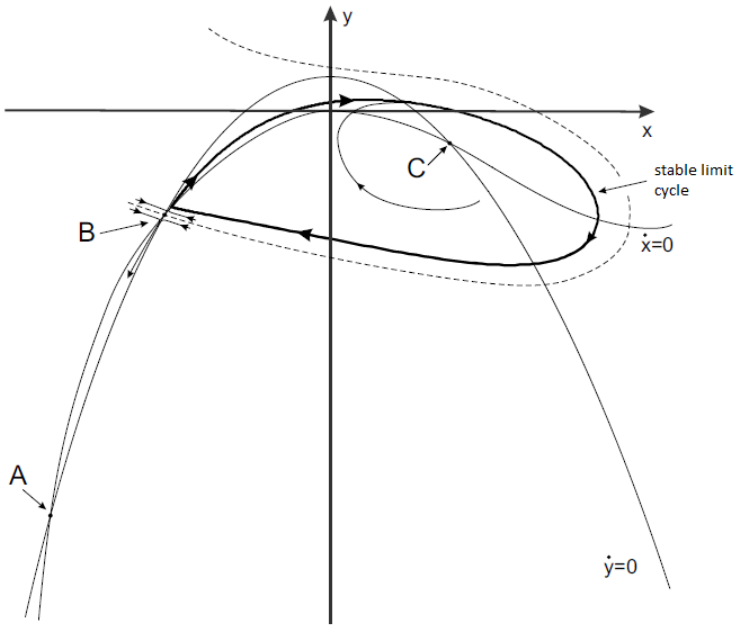

Figure 5: Description for Hindmarsh-Rose model phase plane. The equilibrium points A, B, and C can be a stable node, an unstable saddle, and an unstable spiral, correspondingly, a humble form of f(x) can be used in equation as is pointed out $\dot{\boldsymbol{x}} = \mathbf{0}$ null-cline shows (Steur 2006).

The steady point in the figure (5) is the node A that corresponds to the neuron resting state. By using current pulse de-polarizing that is large enough, $\dot{\boldsymbol{x}} = \mathbf{0}$ null-cline going to be lowered so that the nodes A and B meets and vanishes. Still, the fire ending is impossible by just terminating the stimulus and the state will get out of the limit cycle only after applying a suitable hyper-polarizing pulse. Therefore, to terminate the firing state of the model the term z was inserted. The variable that's been additive stands for a slowly changed current, changing the inserted current I to the effective input I - z. When the neuron in a firing state the z value is requires to be raised. After this modification, the general set of equations for HR model is as shown next:

$$\dot{x} = -x^3 + 3x^2 + y + I - z \qquad (29)$$

$$\dot{y} = 1 - 5x^2 - y \qquad (30)$$

$$\dot{z} = r(h(x) - z) \qquad (31)$$

Notes that the f(x) and g(x) are removed and been substituted by their equivalents. Where x indicates potential of membrane, y denotes the recovery parameter, and z stands for the current adaptation with time constant r. Parameter z rises up through fire state and goes down through the non-fire state. What made the model able to show bursting, chaotic bursting and post-inhibitory rebound are variables h and r. (Hindmarsh and Rose 1984; Steur 2006). Figure (6) displays analysis of phase plane of the equation (29) applying more complex form of f(x) as suggested in (Hindmarsh and Rose 1984).

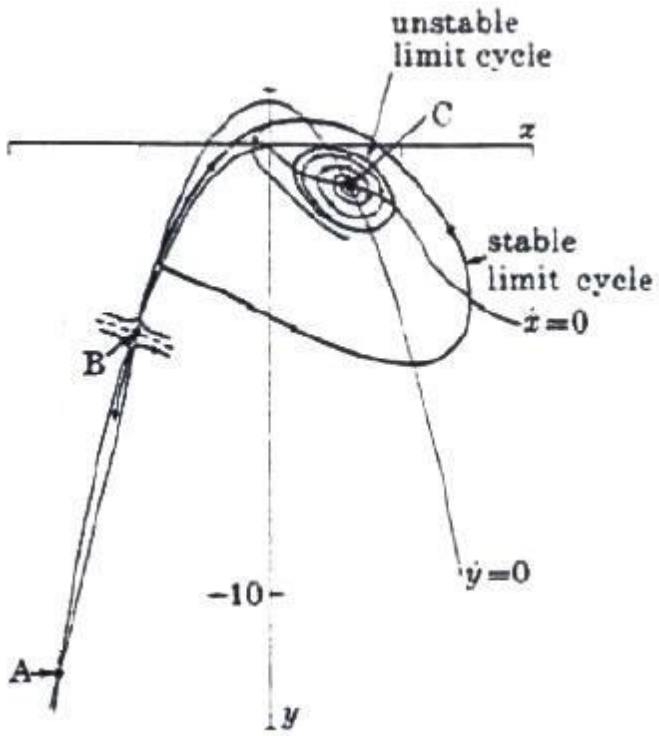

Figure 6: Rose Hind marsh Model about Phase plane representation by using a complex form of f(x). The equilibrium points A, B and C is a static node, an unstable saddle, and an unstable spiral, respectively. Unstable limit cycle is specified here (Rose and Hindmarsh 1984).

3.3 The (DSM) Neuron Model

The Dissipative Stochastic Mechanics based (DSM) neuron has a distinctive formulation that comes from a point of view that conformational changes in ion channels are exposed two different types of noise. Both of these types of noise were coined as the intrinsic noise and topological noise. The intrinsic noise comes from voltage dependent movement of gating particles between the inner and also the outer faces of the membrane which is stochastic; therefore, gates open and close in a probabilistic fashion, that is, it's the average number, not the precise number, of open gates over the membrane which can be specified by the voltage. The topological noise however stems from the existence of a multiple number of the gates inside the channels and is assigned to the fluctuations in the topology of open gates, instead of the fluctuations in the number of open gates.

The next one is the topological noise that originates from multiple numbers of gates existences within the channels and plays a role in the open gates topology, rather than the changes in the open gates number.

Curiously, as gating particles throughout the dynamics usually do not follow a specific order for that occupation of the available closed gates, and also the open gates, the membrane at two distinct times might have an equivalent number of gates being open but two various conductance values. The topological noise is contributed towards the suspicion in the open channels numbers occurring even when open gates numbers are precisely known. Therefore, in defining the dynamics of the voltage, all permits from the gates open topologies that ought to be thought of. DSM neuron formula was created

depending on Hindmarsh-Rose model (Hindmarsh and Rose 1984) and utilizes the Nelson's stochastic mechanics (Nelson 1966 and 1967), within the dissipation existence, to model the ion channel noise impacts about the membrane voltage dynamics. The topological noise influence on the neuron dynamics gets to be more crucial in membranes which are small in size. Accordingly, the DSM neuron functions like the Hindmarsh-Rose model if the membrane size is large.

The motion equations for both variables cumulants are resulted through the formalism from the DSM neuron. The second cumulants that depict the neuron's diffusive manners usually do not concern us within this thesis. The first cumulants develop harmoniously using the dynamics below:

$$m\dot{X} = \Pi + S_5 I \tag{32}$$

$$\dot{\Pi} = -\left(\frac{3a}{m}X^2 - \frac{2b}{m}X + S_0\right)(\Pi + S_5 I) - S_1 a X^3 + S_2 X^2 + S_6 X - S_3 X_{eq}(I) + S_1 I + S_7 - (1-r)[k\left(1 - \frac{\varepsilon_m^y}{m}\right)z + (1-k)\left(1 - \frac{\varepsilon_m^z}{m}\right)y \tag{33}$$

$$\dot{y} = -y - dX^2 + c + n^y \tag{34}$$

$$\dot{z} = -rz + rh(X - x_s) + n^z \tag{35}$$

$$\Pi(t_0) = y(t_0) - z(t_0) - a\left(X(t_0)\right)^3 + b\left(X(t_0)\right)^2 + (1 - S_5)I(t_0) \tag{36}$$

where X indicates the membrane voltage value expected, and Π matches towards the arithmetic mean of the momentum-like operator. Variables y and z describe the short and also the slower ion dynamics, respectively. I represent the outside current inserted in to the neuron, and m represents the capacitance on the membrane. The variables a, b, c, d, r, and h are constants. K is really a mixing coefficient presented by k = 1/(1+r). S_i are constants as shown next:

$$S_0 \coloneqq k + (1-k)r \tag{37}$$

$$S_1 \coloneqq S_0 - [k\frac{\varepsilon_m^y}{m} + (1-k)r\frac{\varepsilon_m^z}{m} \tag{38}$$

$$S_2 \coloneqq k\left(1-\frac{\varepsilon_m^y}{m}\right)(b-d) + (1-k)\left(1-\frac{\varepsilon_m^z}{m}\right)(rb-d) \tag{39}$$

$$S_3 \coloneqq k\varepsilon_u^y + (1-k)\varepsilon_u^z \tag{40}$$

$$S_4 \coloneqq k\frac{\varepsilon_m^y}{m} + (1-k)\frac{\varepsilon_m^z}{m} \tag{41}$$

$$S_5 \coloneqq 1 - S_4 \tag{42}$$

$$S_6 \coloneqq S_3 - S_5 rh \tag{43}$$

$$S_7 \coloneqq (rhx_s + c)S_5 \tag{44}$$

Eq. (36) defines Π value at the beginning time t_0 in terms of the beginning values of the other dynamical parameters *X*, *y* and *z*, and the current *I*. *Xeq(I)* bows to the equation:

$$\mathfrak{a}X_{eq}^3 - (b-d)X_{eq}^2 + h\left(X_{eq} - x_s\right) - c - I = 0 \tag{45}$$

Where x_s is a constant. n^y and n^z in Eqs. (34) and (35) are noises from the Gaussian white kinds with zero means and mean squares presented by:

$$< n^y(t)n^y(t') >= 2mT\delta(t-t') \tag{46}$$

And

$$< n^z(t)n^z(t') >= 2rmT\delta(t-t') \tag{47}$$

are obtained by the fluctuation-dissipation classical theorem. T Indicates a temperature like value. The renormalization terms are the conditions with the correction coefficients $\mathcal{E}_m^y$,$\mathcal{E}_u^y$, $\mathcal{E}_m^z$ and $\mathcal{E}_u^z$ that occur in the equations above, all the parameters in this model are in dimensionless unit.

When the epsilon values reaches values that are larger than (ε_m^y=0.3, ε_u^y=1.5, ε_m^Z=0.003, and ε_u^Z=0.015) that is when the neuron reach the saturation states.

When the noise parameters n^y and n^z are neglected and setting all of the correction coefficients to zero, the dynamics from the DSM works such as dynamics of Hindmarsh-Rose. All of the model parameters, even time, have been in dimensionless units. The initial voltage time number of the membrane for Hindmarsh-Rose's original model is shown within the Figure (7) for many different constant current inputs. Hindmarsh-Rose model dynamical states are quiescence, bursting (rhythmic using a periodicity in high degree, or chaotic), and tonic firing.

It was shown that the representation of intrinsic noise will get to be more important in small size membranes and it's the same in case of fewer channels in DSM Neuron (Güler 2008). The intrinsic noise can be the source of spiking activity in quiet deterministic model and in large input current values bursting can be caused. In figure (8) the DSM Neuron dynamics in a small size membrane is demonstrated. Notice that renormalization corrections are equal to zero so that the result is studied regardless of the topological noise influence.

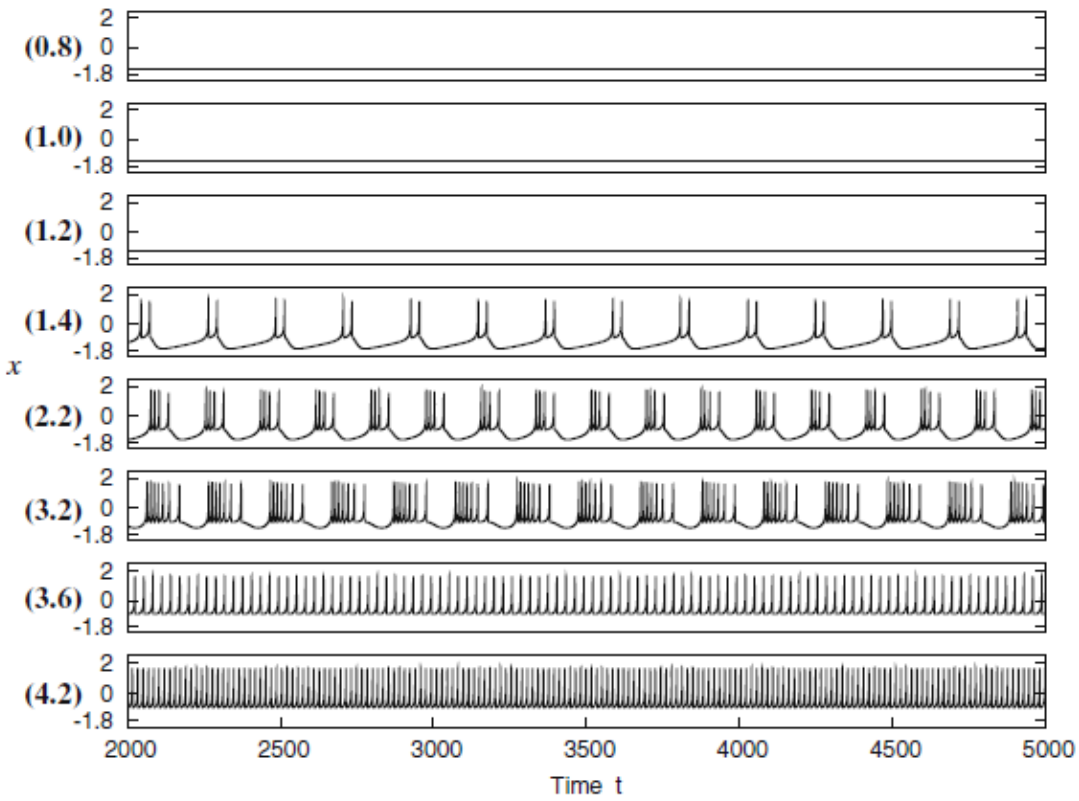

Figure 7: Membrane voltage time series of the deterministic Hindmarsh-Rose model applying the parameter values m = 1, a = 1, b = 3, c = 1, d = 5, h = 4, r = 0.004 and x_s=-1.6; for different constant inputs current values *I*, indicated in a parenthesis on the left of each plot (Güler 2008).

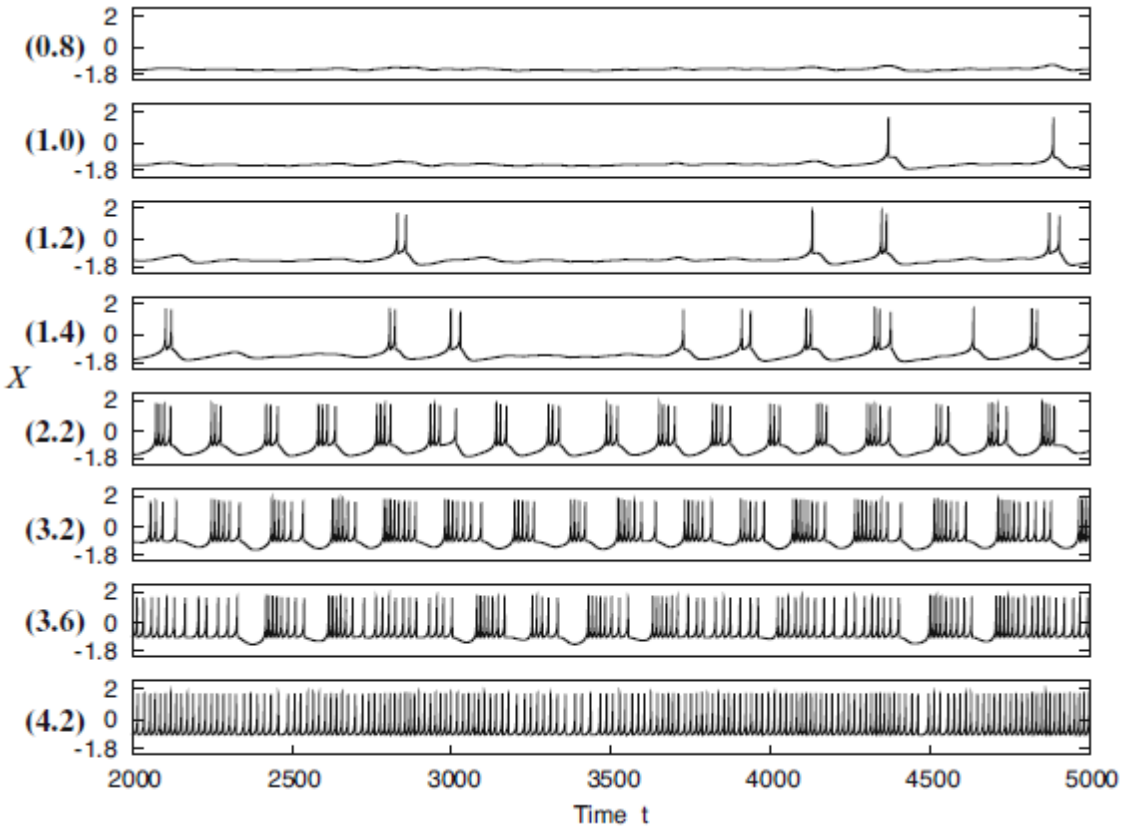

Figure 8: Time series of X when the DSM neuron is exposed just to the intrinsic noise applying the Hindmarsh-Rose $m = 0.25$, $a = 0.25$, $b = 0.75$, $c = 0.25$, $d = 1.25$, $h = 1$, $r = 0.004$ and $\boldsymbol{x_s}$=-1.6 with the temperature $T = 0.008$. Schemes for different constant inputs current values $4I$ (scaled by the factor of four) (Güler 2008).

Renormalization corrections are caused by the interaction between the topological and intrinsic noises. The existence of correction's parameters further increases the shift in behavior from quiescence to spiking and from tonic firing to bursting to a significant degree and with evidence to this; it causes the bursting activity to occur in a wider domain of input currents. Hence, in the existence of the correction terms, the spiking activity begins to occur at smaller input current values and the bursting activity is extended for higher input current values. The DSM neuron manner under the effect of corrections is displayed next page in figure (9).

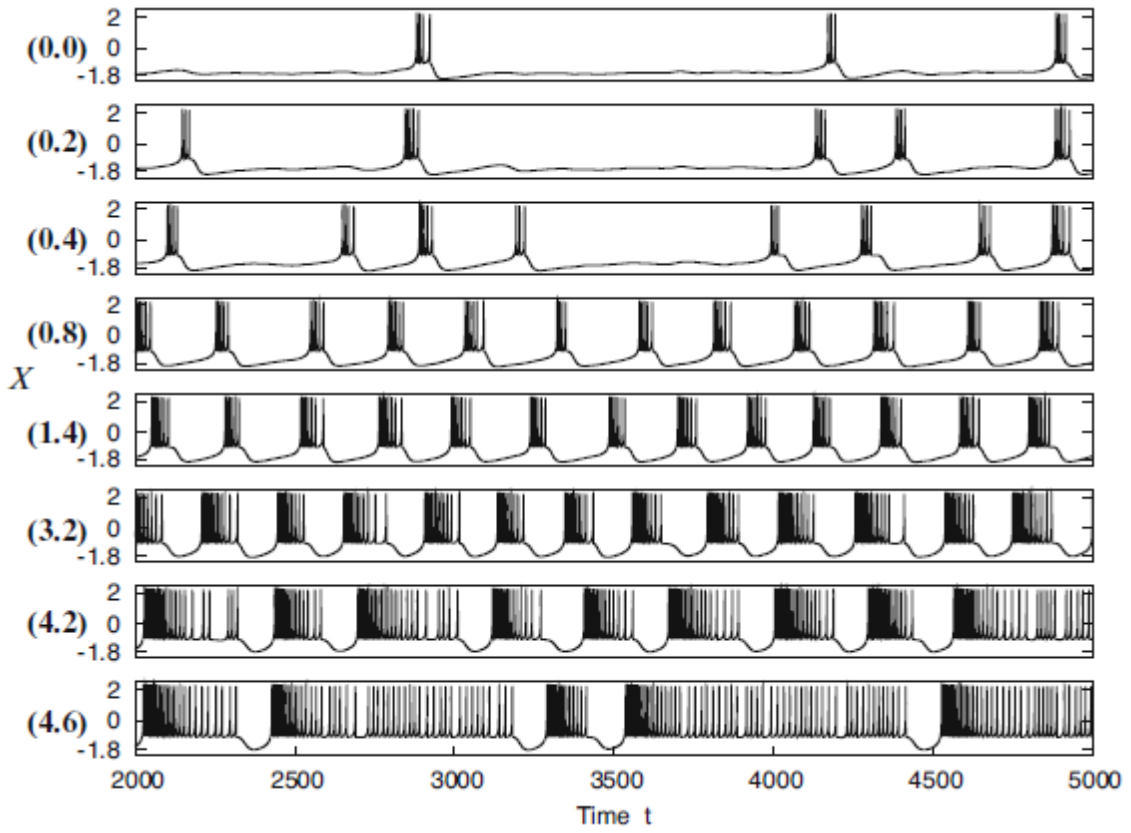

Figure 9: Time series of X using the correction coefficients $\boldsymbol{\varepsilon_m^y = 0.1}$, $\boldsymbol{\varepsilon_u^y = 1.0}$, $\boldsymbol{\varepsilon_m^z = 0.001}$ and $\boldsymbol{\varepsilon_u^z = 0.005}$ with the temperature T = 0.008. The Hindmarsh-Rose parameter are m = 1, a = 1, b = 3, c = 1, d = 5, h = 4, r = 0.004 and $\boldsymbol{x_s}$=-1.6 (Güler 2008).

3.4.1 Noise in neuronal information processing

Noise can enhance neuronal systems from signal transmission properties point of view under certain conditions. Sub-threshold oscillations in a neuron may have an important effect on the data coding in neurons when magnified by noise (Braun 1998). The perfect noise amount existence in the neuron system may have association with the input signal to enhance signal observation (Gerstner and Kistler 2002).

There are two types of noise; the internal and external which have been explained within the DSM neuron approach model in the third chapter. In this study the noise is a white

Gaussian noise and considered to be one variable containing both the internal and the external noise.

Gaussian noise is statistical noise that has its probability density function equal to that of the normal distribution, which is also known as the Gaussian distribution. In other words, the values that the noise can take on are Gaussian-distributed. A special case is white Gaussian noise, in which the values at any pairs of times are statistically independent (and uncorrelated). In applications, Gaussian noise is most commonly used as additive white noise to yield additive white Gaussian noise.

Chapter 4

NUMERICAL EXPERIMENTS

4.1 The Role Played by the Renormalization Terms in neurons

In our investigation we examine the role played by the renormalization terms and to be exact the effect of the epsilons value on the neuron. We change the epsilons values many times and compare between them to see the epsilons values on the neuron.

The model's behavior is studied within the following ranges of the parameters: We used input current values between (1-7) and the other experiments the input current was (7-11). In the first experiment the default epsilons values as in Label (A) in Table (1) is used and by changing the input current from (1-7) we get the first set of result, after that we used the epsilons values as in Label (B) in Table (1) and did the experiment again to get the second set of result and finally we make the epsilons values equal to zero as in Label (K) in Table (1) and did the experiments again so we can get the third set of result to draw the result that in the figure (10) below.

After that we change the default epsilons values and take four new epsilons values that will replace the default epsilon value in the first experiment. The first two epsilon values are smaller than the default epsilon values and there values are multiplied be 0.5 and 0.8 as in Table (1) (Label C and E respectively), we draw the three result while changing the

input current, the first set when the epsilon values are zero as in Label (K) in Table (1),the second set when the default epsilon value are multiplied by 0.5 and 0.8 as in Table (1) (Label C and E respectively) and the last set when we used epsilon values as in Label (C) in Table (1) and we collected the result as in the figures (12) and the figure (14) for the default epsilon value as in Label (E) in Table (1).

Now the second two epsilon values which are larger than the default epsilon values and there values are calculated by multiplied the default epsilon value be 1.3 and 1.5 and there values are in Table (1) (Label G, I respectively), the first set of result is calculated when the epsilons values are zero as in Label (K) in Table (1), the second set when the default epsilon value are multiplied by 1.3 and 1.5 as in Table (1) (Label G, I respectively), the last set of result when we used the epsilons values as in Label (H) in Table (1) the results are drown in the figure (16) and figure (18) for the default epsilon value when we used it as in Label (J) in Table (1).

Table 1: Parameter sets of the epsilon values used in the thesis.

LABEL	Multiply the default by	ε_m^y	ε_u^y	ε_m^Z	ε_u^Z
A	Default (0.1)	0.1	0.5	0.0001	0.0005
B	Double (0.1)	0.2	1	0.0002	0.001
C	0.5	0.05	0.25	0.0005	0.0025
D	Double (0.5)	0.1	0.5	0.001	0.005
E	0.8	0.08	0.4	0.0008	0.004
F	Double (0.8)	0.16	0.8	0.0016	0.008
G	1.3	0.13	0.65	0.0013	0.0065
H	Double (1.3)	0.26	1.3	0.0026	0.013
I	1.5	0.15	0.75	0.0015	0.0075
J	Double (1.5)	0.3	1.5	0.003	0.015
K	Zero	0	0	0	0

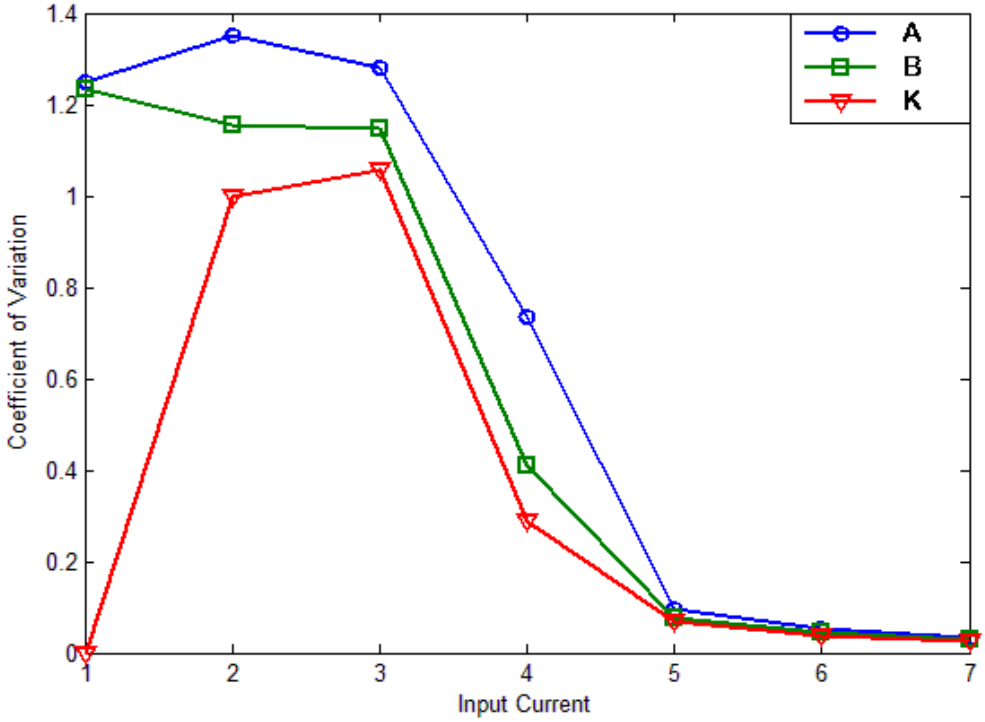

Figure 10: The Coefficient of Variation against the Input Current. The Three Plots are Shown the Labels (A), (B), and (k) Parameters as in the Table (1).

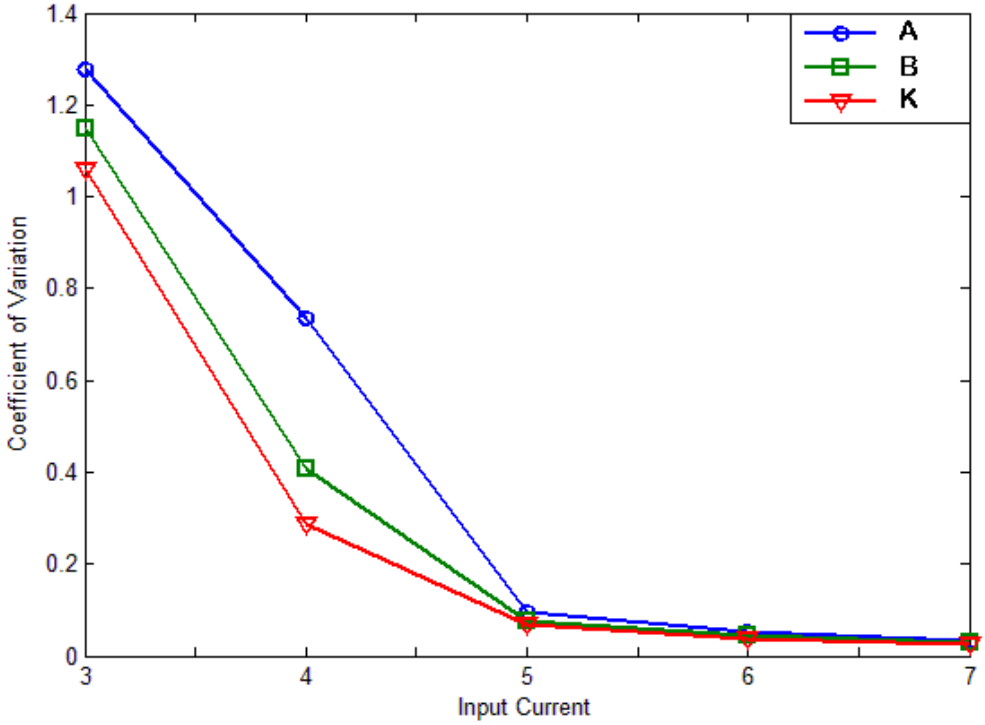

Figure 11: The Coefficient of Variation against the Input Current. The Three Plots are Shown the Labels (A), (B), and (k) Parameters as in the Table (1).

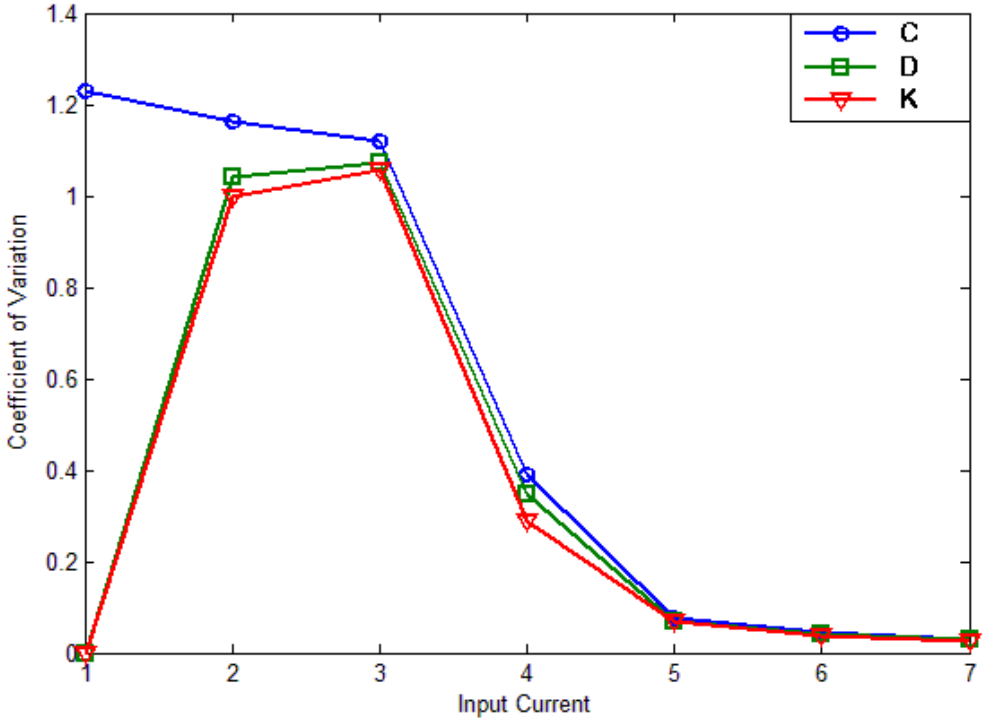

Figure 12: The Coefficient of Variation against the Input Current. The Three Plots are Shown the Labels (C), (D), and (k) Parameters as in the Table (1).

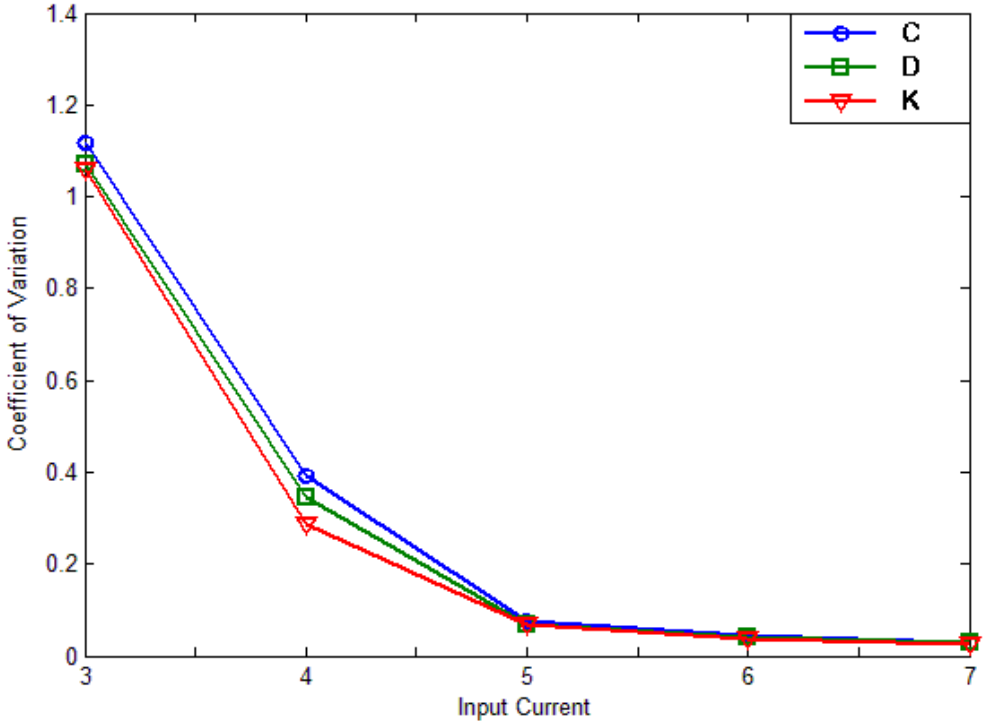

Figure 13: The Coefficient of Variation against the Input Current. The Three Plots are Shown the Labels (C), (D), and (k) Parameters as in the Table (1).

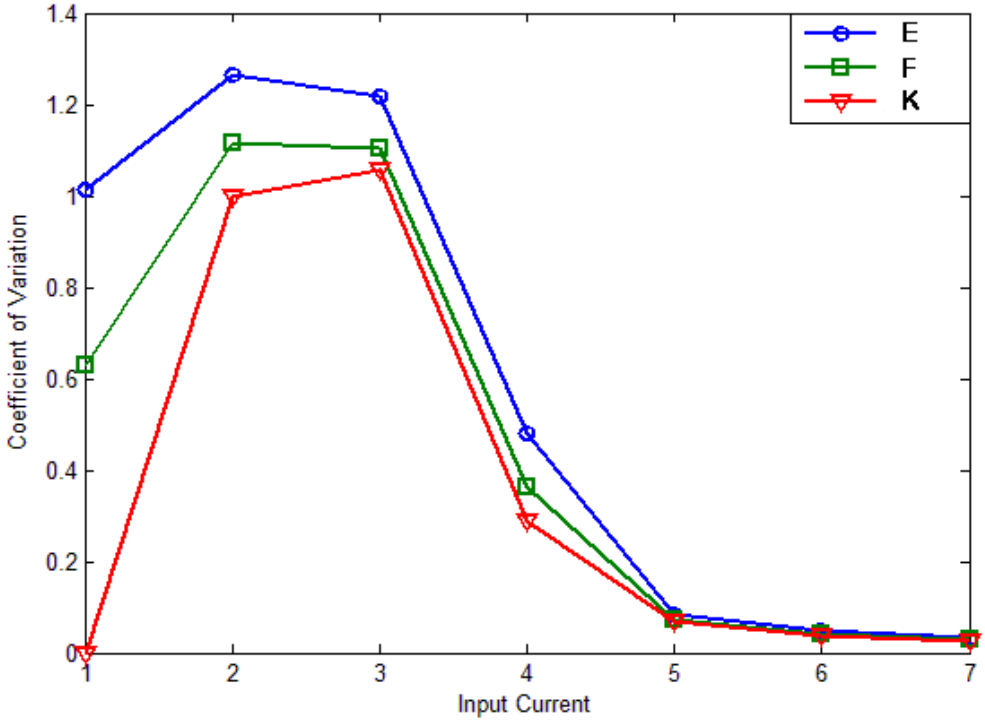

Figure 14: The Coefficient of Variation against the Input Current. The Three Plots are Shown the Labels (E), (F), and (k) Parameters as in the Table (1).

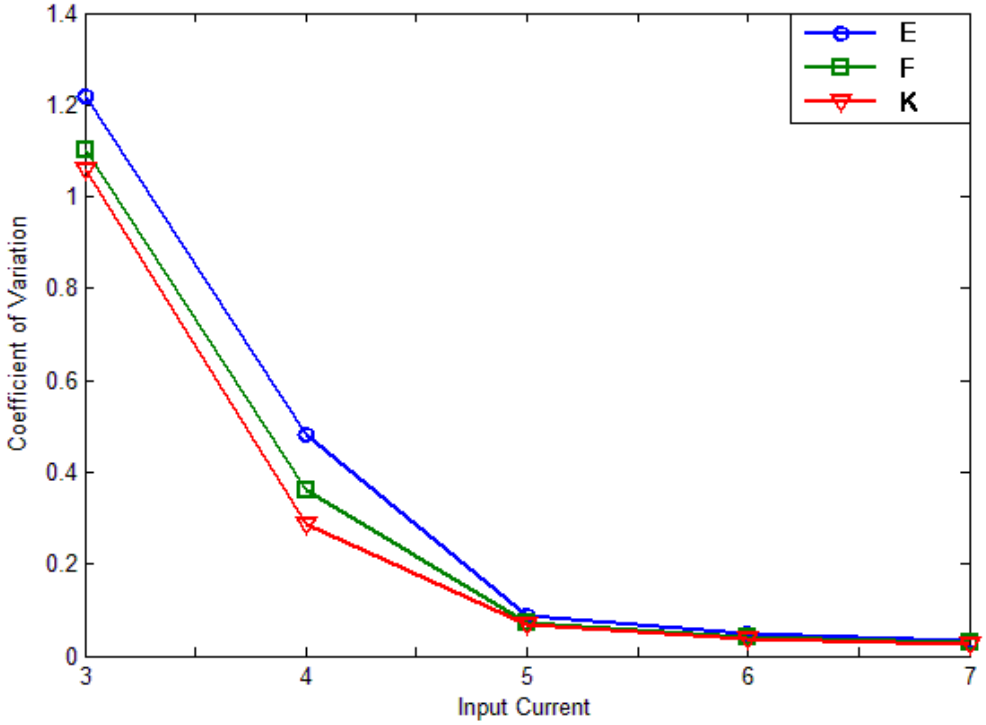

Figure 15: The Coefficient of Variation against the Input Current. The Three Plots are Shown the Labels (E), (F), and (k) Parameters as in the Table (1).

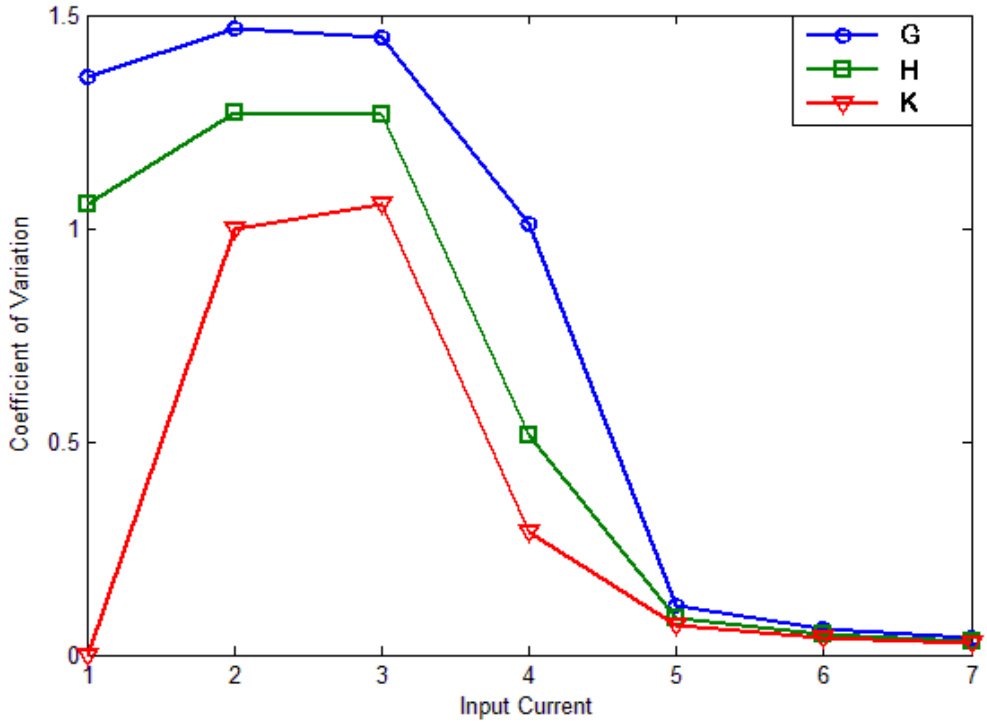

Figure 16: The Coefficient of Variation against the Input Current. The Three Plots are Shown the Labels (G), (H), and (k) Parameters as in the Table (1).

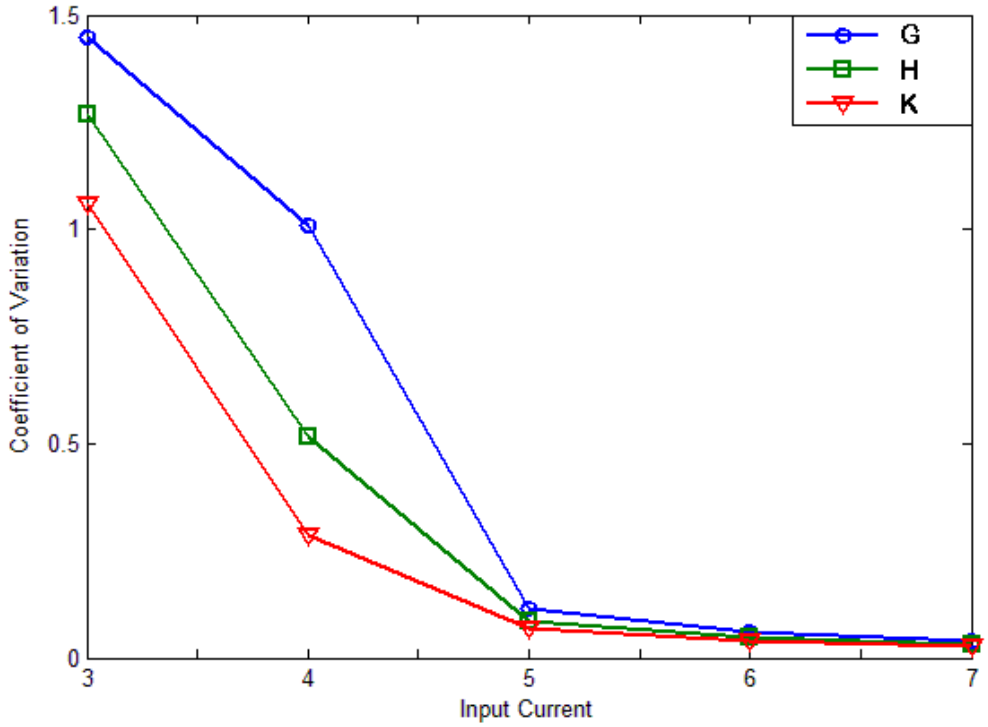

Figure 17: The Coefficient of Variation against the Input Current. The Three Plots are Shown the Labels (G), (H), and (k) Parameters as in the Table (1).

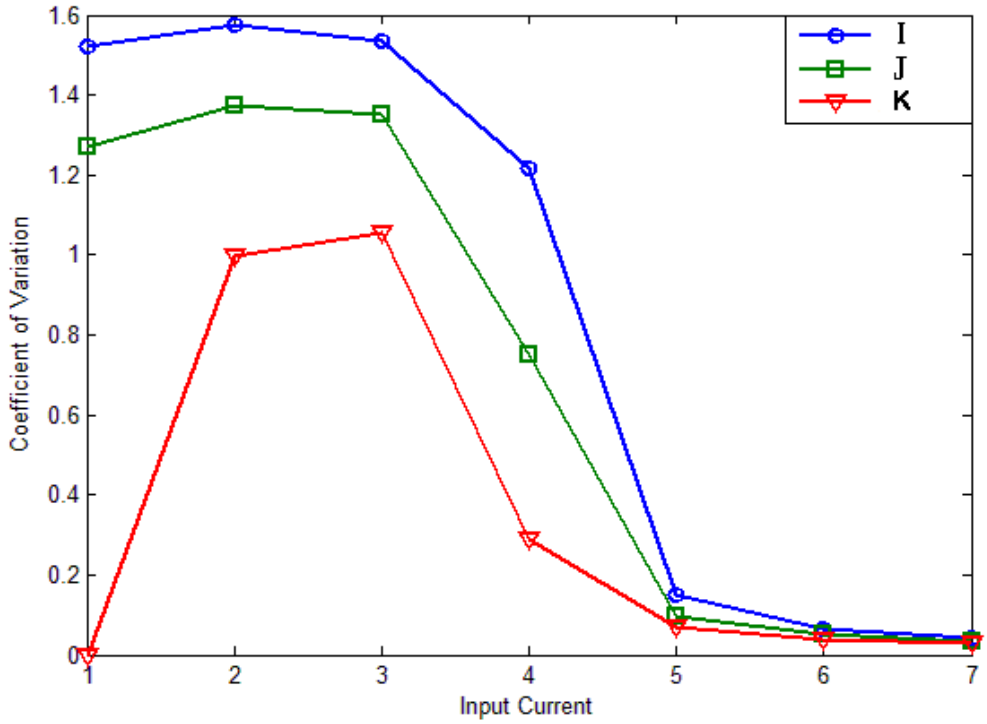

Figure 18: The Coefficient of Variation against the Input Current. The Three Plots are Shown the Labels (I), (J), and (k) Parameters as in the Table (1).

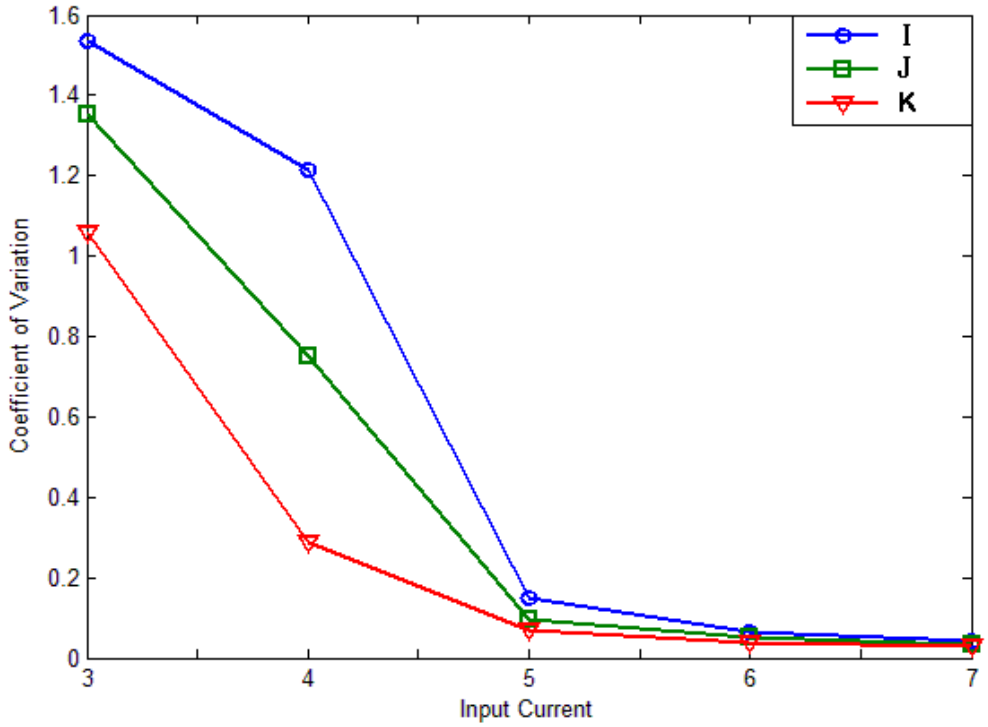

Figure 19: The Coefficient of Variation against the Input Current. The Three Plots are Shown the Labels (I), (J), and (k) Parameters as in the Table (1).

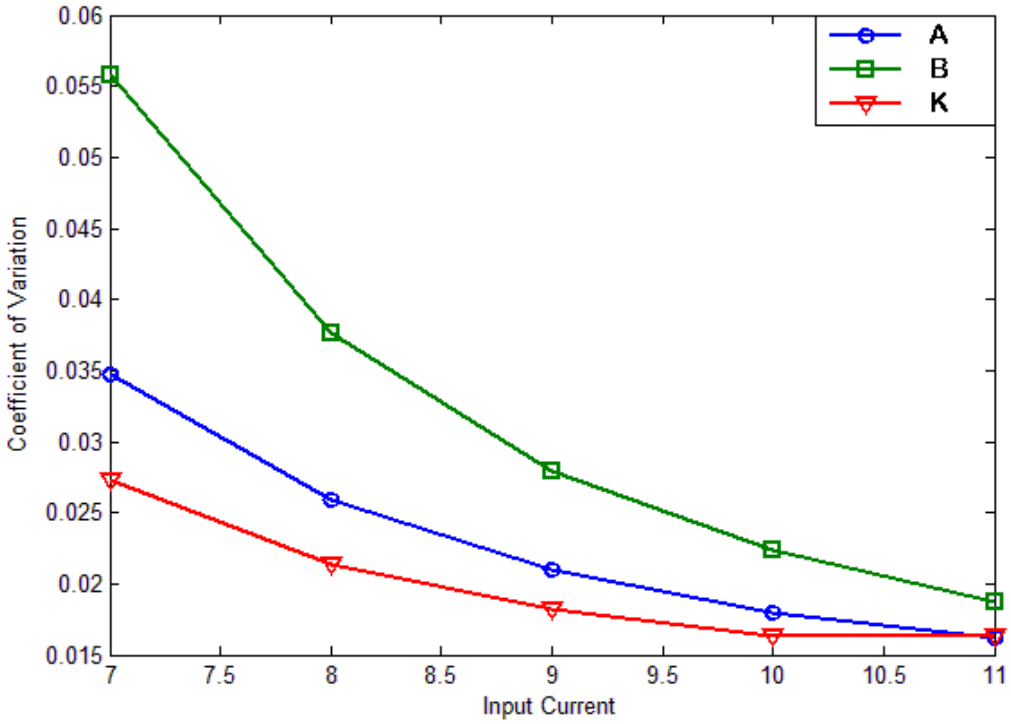

Figure 20: The Coefficient of Variation against the Input Current. The Three Plots are Shown the Labels (A), (B), and (k) Parameters as in the Table (1).

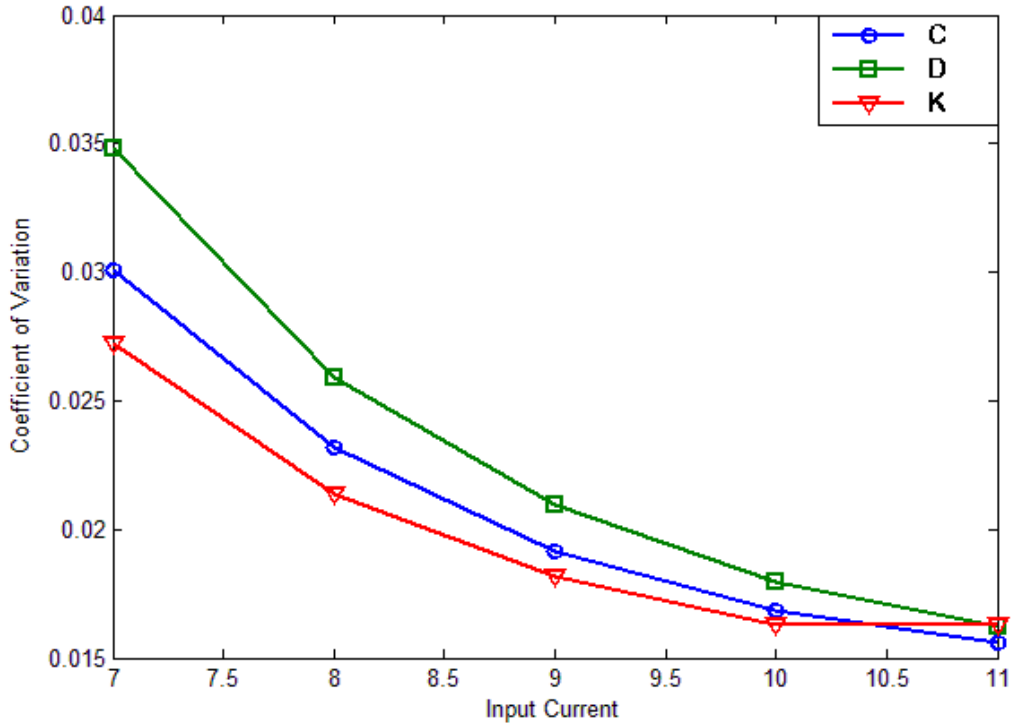

Figure 21: The Coefficient of Variation against the Input Current. The Three Plots are Shown the Labels (C), (D), and (k) Parameters as in the Table (1).

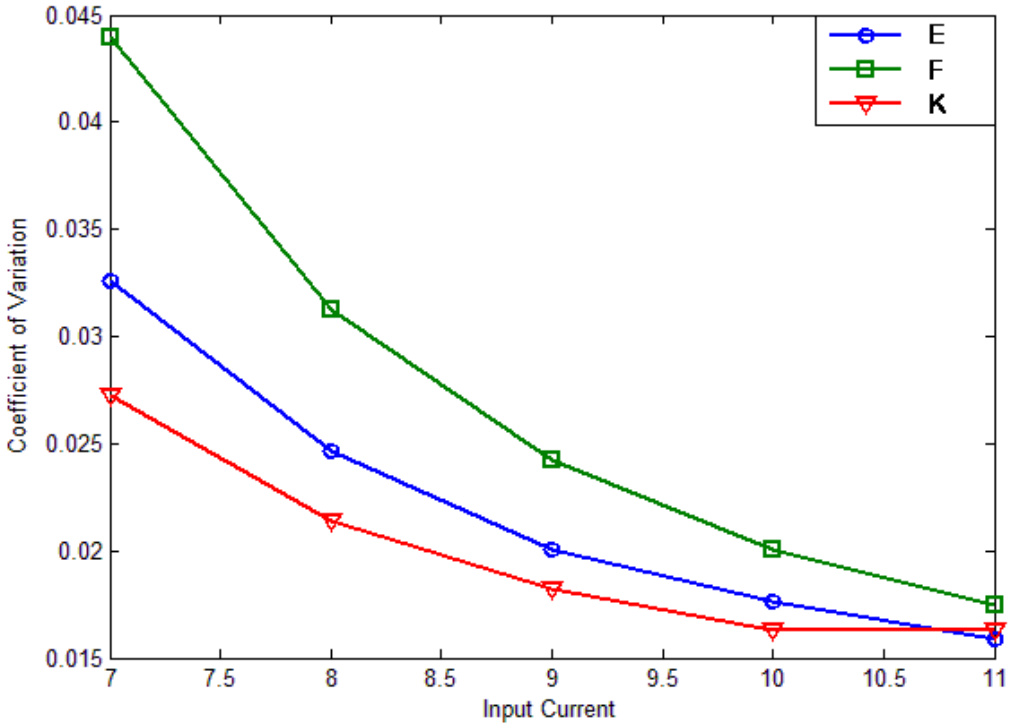

Figure 22: The Coefficient of Variation against the Input Current. The Three Plots are Shown the Labels (E), (F), and (k) Parameters as in the Table (1).

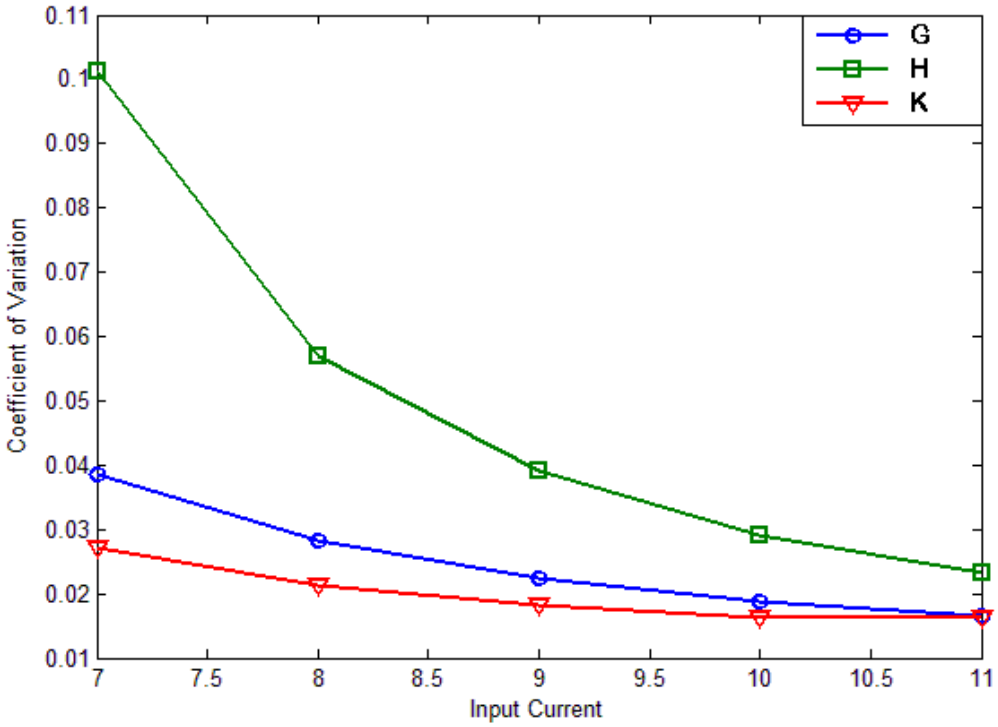

Figure 23: The Coefficient of Variation against the Input Current. The Three Plots are Shown the Labels (G), (H), and (k) Parameters as in the Table (1).

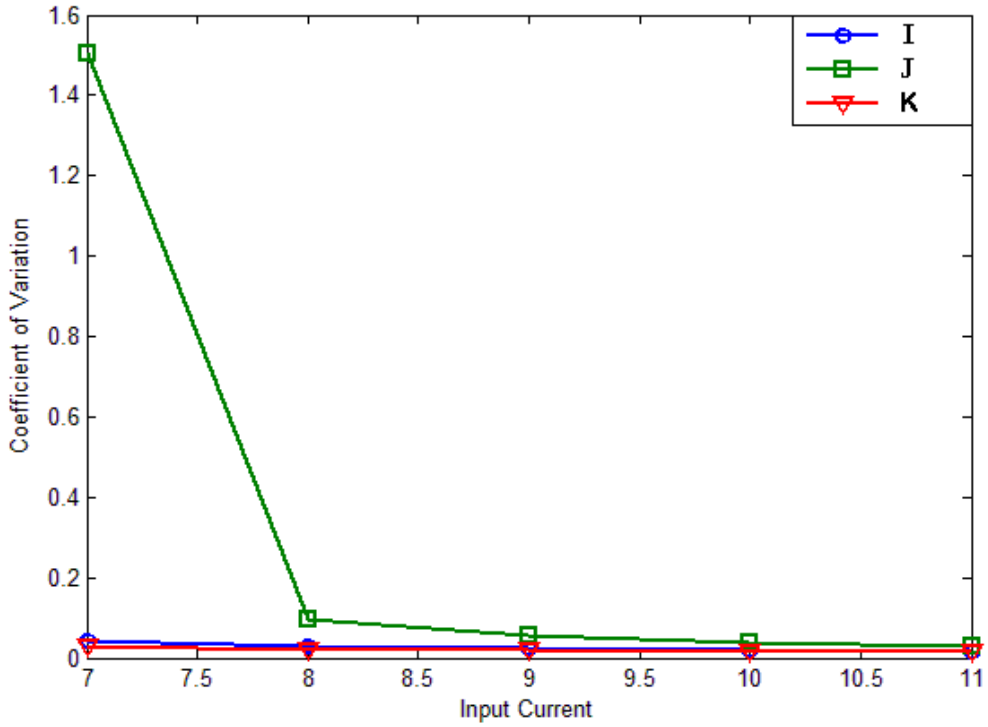

Figure 24: The Coefficient of Variation against the Input Current. The Three Plots are Shown the Labels (I), (J), and (k) Parameters as in the Table (1).

In the experiments in figures (10 to 19) the input current was from (1-7) and because of that the effect of the epsilon values makes the double epsilon values to go under the defualt epsilon values. When we compare the default epsilon values in figure (10) with the two epsilon values that are smaller than the defualt epsilon values that we got the first epsilon values as in Label (C) in Table (1) and the second epsilon values as in Label (E) in Table (1) the epsilon values effect will start reducing. However, when we compare the default epsilon values as in figure (10) with the two epsilon values larger than the default epsilon values will be in the first one as in the Label (G) in table (1) as in figure (16) and the second one will be as in Label (I) in Table (1) as in the figure (18) the effect of the epsilon values will start to increase as the epsilon values increase.

After that we change the input current from (1-7) to (7-11) and compare the default epsilon value in figure (20) with the two epsilon values smaller than the default epsilon value as in Label (C , E) in Table (1) for figure (21) and figure (22) respectivly we found out that the influence of the epsilons values was reduced compere with default value. After that when we compare the default epsilon value in figure (20) with the other two epsilons values that are larger than the default epsilon value which we have them from the Label (G , I) in Table (1) for figure (23) and figure (24) respectivly and the input current from (7-11) we realized that the impact of the epsilons values start to increase and that makes the neuron lose its properties and after a while when the increase the epsilon values higher the neuron starts to become ineffective until the increase passes the value ($\varepsilon_m^y = 0.15$, $\varepsilon_u^y = 0.75$, $\varepsilon_m^z = 0.0015$, and $\varepsilon_u^z = 0.0075$) when its double reaches values that are larger than ($\varepsilon_m^y = 0.3$, $\varepsilon_u^y = 1.5$, $\varepsilon_m^z = 0.003$, and $\varepsilon_u^z = 0.015$) when the neuron reachs the saturation states.

Our result shows that we the default epsilon value is much better to be use when dealing with the DSM neuron.

4.2 Technologies Used in this Thesis

The DSM neuron model has been developed by Prof. Marifi Güler in C++ and some code has been changed like the main equation in the models in order to make it possible to do the experiments of this thesis. The model has been written by the C++ language. The GnuPlot program was used to plot the results and voltage time series.

Chapter 5

CONCLUSION

In this thesis, the DSM neuron model was investigated from a numerical point of view when exposed to renormalization terms. The impacts of the epsilon values on the neuron were checked. Correction coefficients were used as an effective measure of renormalization corrections to the model. It should be considered that these renormalization corrections appear from the dilemma of being in doubt of how many open ion-channel numbers there are, even if we know the exact number of open gates.

DSM model neurons appear to be more complex than other models. It shows quicker synchronizing between two DSM neurons (Jibril and Güler 2009), dynamics of the models under constant input currents (Güler 2008) and in addition, its ability in detecting signals under noise varying and periodic input currents, that have been inspected during this study, are all the model benefits that deserve tolerating the complexity of it. Furthermore, it should be taken into consideration that this model is extremely capable of handling the small membrane sizes of the neurons.

The experiment show that the renormalization terms effects play a role on the value of coefficient of variation for a small input current but for large input current there is no effect.

The epsilon values shown when the input current are large, there is no effect because the spike increasing high, so between two spike events the renormalization effect do not have time to show themselves because before the time show the effect, another spike start. But when the input current is small the spike low, so there is a stabile time for renormalization to show the effect.

The experiments show that the epsilon values plays important role. The absence of the epsilon values makes the neuron generate spikes in slow manner and makes it have the lowest coefficient of variation.

The existence of the epsilon values when the input current is higher than (7) makes the neuron react better and have higher coefficient of variation compare to the case when the epsilon value equal to 0 as in figures (20 to 24).

(10 to 19) show that when the input current is lower than (7) the neuron react the same as before however it defer only when we double the epsilon values it result will goes under the result of the default value because of the effect of the epsilon values.

The results reveal that the neurons are extremely able to make a complicated and advantageous use of the channel noise in handling signals. From a technological point of view, the study shows that the DSM model has promising potential for signal detection.

REFERENCE

Abdulmonim M. N., An Investigation into the Dissipative Stochastic Mechanics Based Neuron Model under Input Current Pulses, MS 2013.

Almassian A., An Investigation into the DSM Neuron Model under Time Varying Input Currents, MS 2011.

Braun H.A., Huber M.T., Dewald M., Sch¨afer, K., and Voigt, K., Computer simulations of neuronal signal transduction: The role of nonlinear dynamics and noise. Int. J. Bif. Chaos 8, 881–889, 1998.

Chow C. C. and White J. A., Spontaneous action potentials due to channel fluctuations. Biophys. Journal 71: 3013-3021, 1996.

Dayan P. and Abbot L. F., Theoretical Neuroscience Computational and Mathematical Modeling of Neural Systems, MIT Press, 2002.

DeFelice, L. J., Chaotic states in a random world: Relationship between the nonlinear differential equations of excitability and the stochastic properties of ion channels. Journal of Statistical Physics, 70, 339–354, 1992.

Faisal, A. A., Stochastic simulations on the reliability of action potential propagation in thin axons. PLoS Computational Biology, 3, e79, 2007.

Faisal A. A., Selen L. P. J., and Wolpert D.M., Noise in the nervous system. Nature Revs. Neurosci. 9:292–303, 2008.

FitzHugh R., Nagumo j. .Impulses and physiological states in theoretical models of nerve membrane. Biophysical J. 1:445-466, 1961.

Fox R. F. and Y.N. Lu, Emergent collective behavior in large numbers of globally coupled independently stochastic ion channels. Phys. Rev. E, 49: 3421-3431, 1994.

Gerstner W., Kistler W., Spiking Neuron Models, Single Neurons, Populations, Plasticity, Cambridge University Press, 191, 2002.

Güler M., Modeling the effects of channel noise in neurons: A study based on dissipative stochastic mechanics. Fluct. Noise Lett. 6:L147-L159, 2006.

Güler M., Dissipative stochastic mechanics for capturing neuronal dynamics under the influence of ion channel noise. Phys. Rev. E, 76, 041918(17), 2007.

Güler M., Detailed numerical investigation of the dissipative stochastic mechanics based neuron model. J. Comput. Neurosci. 25:211–227, 2008.

Güler, M., Persistent membranous cross correlations due to the multiplicity of gates in ion channels. Journal of Computational Neuroscience ,31,713-724, 2011.

Güler M., Stochastic Hodgkin-Huxley equations with colored noise terms in the conductances. Neural Computation. 25:46-74, 2013.

Hodgkin, A.L. &Huxley, A.F. .A quantitative description of membrane current and its application to conduction and excitation in nerve. Journal of Physiology (London. Print), 117, 500–544, 1952.

Hindmarsh J.L. and Rose R.M., A model of neuronal bursting using three coupled first order differential equations. Proc. R. Soc. Lond. B Biol. Sci. 221, 87–102, 1984.

Jacobson G. A. et al., Sub-threshold voltage noise of rat neocortical pyramidal neurons. J. Physiology 564: 145-160, 2005.

Jassim H. M., An Investigation into the Dissipative Stochastic Mechanics Based Neuron Model under Noisy Input Currents, MS 2013.

Jibril G. O. and Güler M., The renormalization of neuronal dynamics can enhance temporal synchronization among synaptically coupled neurons. Proc. Int. Joint Conf. on Neural Networks, 1433-1438, 2009.

Jung, P. &., Optimal sizes of ion channel clusters. Europhysics Letters, 56, 29–35, 2001.

Kole M. H., Hallermann S., and Stuart G. J., Single Ih channels in pyramidal neuron dendrites: properties, distribution, and impact on action potential output. J. Neurosci., 26: 1677-1687, 2006.

Kolb B. and Whishaw I. Q., Fundamentals of Human Neuropsychology, Sixth Edition, Worth Publishers, 4: 83, 91, 92, 2009

Lu, F. R., Emergent collective behavior in large numbers of globally coupled independently stochastic ion channels, 1994.

Nagumo J., Arimoto S., and Yoshizawa S. (1962) An active pulse transmission line simulating nerve axon. Proc. IRE. 50:2061–2070.

Nelson E., Derivation of the Schrödinger Equation from Newtonian Mechanics, Phys. Rev. 150, 1079, 1966.

Nelson E., Dynamical Theories of Brownian Motion _Princeton University Press, Princeton, NJ, 1967.

Ochab-Marcinek, A. S., Noise-assisted spike propagation in myelinated neurons. Physical Review E, 79, 011904(7), 2009.

Özer, M., Frequency-dependent information coding in neurons with stochastic ion channels for subthreshold periodic forcing. Physics Letters A, 354, 258–263, 2006.

Rose R. M. and Hindmarsh J. L., Amodel of Thalamic neuron, Proceedings of the Royal Society of London. Series B, Biological Sciences, 1984.

Rowat, P. F., State-dependent effects of Na channel noise on neuronal burst generation. Journal of Computational Neuroscience, 16, 87–112, 2004.

Rubinstein, J., Threshold fluctuations in an N sodium channel model of the node of Ranvier. Biophysical Journal,68, 779–785, 1995.

Sakmann B. and Neher N., Single-Channel Recording (2nd ed.) New York: Plenum 1995.

Schmid G., Goychuk I., and Hänggi P., Stochastic resonance as a collective property of ion channel assemblies. Europhys. Lett. 56: 22-28, 2001.

Schneidman E., Freedman B., and Segev I., Ion channel stochasticity may be critical in determining the reliability and precision of spike timing. Neural Comput. 10: 1679-1703, 1998.

Segev I., Cable and Compartmental Models of Dendritic Trees in Bower J. M., Beeman D., The Book of Genesis, 5: 55, 2003.

Steur E., Parameter Estimation in Hindmarsh-Rose Neurons, Traineeship report, 2006.

Strassberg, A. F., Limitations of the Hodgkin–Huxley formalism: Effects of single channel kinetics on transmembrane voltage dynamics. Neural Computation 5, 843–855 , 1993.